Determination of early warning signs for photocatalytic degradation of titanium white oil paints by means of surface analysis

van Driel, B. A.; Wezendonk, T. A.; van den Berg, K. J.; Kooyman, P. J.; Gascon, J.; Dik, J.

DOI
10.1016/j.saa.2016.04.026

Publication date
2017

Document Version
Accepted author manuscript

Published in
Spectrochimica Acta Part A: Molecular and Biomolecular Spectroscopy

Citation (APA)
van Driel, B. A., Wezendonk, T. A., van den Berg, K. J., Kooyman, P. J., Gascon, J., & Dik, J. (2017). Determination of early warning signs for photocatalytic degradation of titanium white oil paints by means of surface analysis. *Spectrochimica Acta Part A: Molecular and Biomolecular Spectroscopy*, *172*, 100-108. https://doi.org/10.1016/j.saa.2016.04.026

http://dx.doi.org/10.1016/j.saa.2016.04.026
Spectrochimica Acta Part A: Molecular and Biomolecular Spectroscopy, vol. 172, 2017

Determination of early warning signs for photocatalytic degradation of titanium white oil paints by means of surface analysis.

B.A. van Driel[a,b,c], T.A. Wezendonk[d], K.J. van den Berg[c], P.J. Kooyman[d,1], J. Gascon[d] and J. Dik[b]

[a] Rijksmuseum, Hobbemastraat 22, 1071 ZC, Amsterdam, The Netherlands
[b] Materials for Arts and Archeology, 3ME, TU Delft, Mekelweg 3, 2628 CD Delft, The Netherlands
[c] Cultural heritage agency of the Netherlands, Hobbemastraat 22, 1071 ZC, Amsterdam, The Netherlands
[d] Catalysis Engineering, ChemE, TU Delft, Julianalaan 136, 2628 BL, Delft, The Netherlands

b.van.driel@rijksmuseum.nl (corresponding author); t.a.wezendonk@tudelft.nl; patricia.kooyman@uct.ac.za; k.van.den.berg@cultureelerfgoed.nl; j.dik@tudelft.nl; j.gascon@tudelft.nl

Abstract

Titanium white (TiO_2) has been widely used as a pigment in the 20th century. However, its most photocatalytic form (anatase) can cause severe degradation of the oil paint in which it is contained. UV light initiates TiO_2-photocatalyzed processes in the paint film, degrading the oil binder into volatile components resulting in chalking of the paint. This will eventually lead to severe changes in the appearance of a painting. To date, limited examples of degraded works of art containing titanium white are known due to the relatively short existence of the paintings in question and the slow progress of the degradation process. However, UV light will inevitably cause degradation of paint in works of art containing photocatalytic titanium white.

In this work, a method to detect early warning signs of photocatalytic degradation of unvarnished oil paint is proposed, using atomic force microscopy (AFM) and X-ray photoelectron spectroscopy (XPS). Consequently, a four-stage degradation model was developed through in-depth study of TiO_2-containing paint films in various stages of degradation. The XPS surface analysis proved very valuable for detecting early warning signs of paint degradation, whereas the AFM results provide additional confirmation and are in good agreement with bulk gloss reduction.

Keywords: Photocatalysis, Titanium dioxide white, Atomic Force Microscopy, X-ray Photoelectron spectroscopy, oil paint, degradation.

1. Introduction

Works of art degrade over time. Society in general, and collection curators specifically, perceive these changes as unwanted. As a result, museums take elaborate precautions to prevent damage to their collection [1]. Unvarnished paintings containing photocatalytic titanium white form a distinct risk group for degradation, since the pigment has the ability to break down the binder through UV light-initiated photocatalysis [2]. Titanium white was first introduced in the 1920s and rapidly became the most widespread pigment of the 20th century. Many famous artists such as Pablo Picasso, Jackson Pollock and Piet Mondriaan have used this pigment [2-4]. Until now, limited examples of degraded works of art containing titanium white have been documented [2, 5-7]. The limited documentation can be the consequence of the slow

[1] Current address: ChemEng, University of Cape Town, Private Bag X3, Rondebosch 7701, South Africa

progress of the degradation process combined with the relatively short existence of the paintings in question. Nonetheless, degradation will inevitably take place if a painting containing photocatalytic titanium white is exposed to UV light [6]. Proper understanding of the degradation process and the development of methods to monitor degradation can provide fundamental information for preventive measures.

The two most commonly used forms of titanium dioxide are rutile and anatase; it is the anatase polymorph that is most photocatalytically active [8-10]. On the other hand, the rutile type is less photocatalytic by nature and additionally, often coated with an inorganic surface layer to further reduce photocatalytic activity [11]. This inorganic coating can consist of different layers of material such as alumina, silica and zirconia [2, 11-13]. In the course of the pigment development in the 20th century, various types of pigments with different properties have reached the market [12]. For instance, production of the rutile type pigment was discovered and implemented since the 1940s [2, 12], and surface coatings were patented from the 1960s onward [13]. Different qualities of surface coatings can be present resulting in different pigment qualities [14]. Properly coated pigments have low to non-existent photocatalytic activity, while still absorbing UV light. Therefore, these pigments can function as UV protectors rather than photocatalysts [15, 16]. Furthermore, uncoated anatase pigments were produced and used in oil paints until far into the 20th century [17]. In this work, we distinguish between two general types of titanium white pigments: photocatalytic pigment (uncoated anatase, UA) and photostable pigment (coated rutile, CR). The photocatalytic pigment is the pigment of interest, while the photostable pigment is used for comparison and to determine if the observed changes can be attributed to photocatalysis or to other degradation events.

Photocatalytic degradation can occur in different forms, depending on the material surrounding the photocatalytic pigment. In general, the degradation reactions are caused by radicals formed on the TiO_2 surface [18-20]. Photocatalytic reactions can cause alteration of surrounding pigments, such as the fading of Prussian blue or alizarin lake (Scheme 1, process 1) [21-23]. On the other hand, degradation of the paint binder can occur by extensive cross-linking, causing embrittlement [16, 24] mainly visible in the form of cracks, or by degradation into volatile components (Scheme 1, process 2 and 3). The current paper focuses on the latter process, more specifically on the degradation of the oil binder (Scheme 1, process 3). This degradation process causes roughening of the surface and eventually leads to chalking: the top layer of the paint has degraded and the pigment is now located freely on the surface [18, 25-27].

(1) *TiO_2 + hv + binder formed by a radical addition polymerization → Further cross-linking leading to embrittlement*

(2) *TiO_2 + hv + colored pigments → change of color due to modification of the chemical structure or oxidation/reduction of inorganic pigments*

(3) *TiO_2 + hv + oil binder → Volatile organic components

Scheme 1: TiO_2 catalyzed degradation processes, process #3, indicated in bold, is the process of interest in this paper.

Chalking of titanium white alkyd paints was first demonstrated by Voltz et al. in 1981 [18]. Scanning electron microscopy (SEM) images showed the morphological differences between a chalked surface caused by photocatalysis and a chalked surface caused by ordinary photo-oxidative degradation. Monitoring the aging of titanium white paints has been performed using several other techniques as well such as weight loss, change of gloss,

Gel Permeation Chromatography (GPC), Fourier Transform Infra Red spectroscopy (FTIR), XPS and AFM [16, 28-33]. Most of this work has been done on modern paint binders and polymeric systems such as alkyds, acrylics and polyalkenes. The aging of oil paint has also been studied widely, but not many papers concerning the effect of titanium white on oil paint aging have been published [34-38].

The main purpose of monitoring the aging of paint films is to gain understanding of the degradation processes, but also to be able to determine whether degradation is taking place before this is visible to the human eye. Investigating the aging of paint films can be performed by monitoring bulk and surface changes. These changes can be classified as optical changes (in the case of chalking, caused by changes in surface morphology of the paint film), chemical changes (in the case of chalking, related to the degradation of oil and the appearance of unbound titanium dioxide), and mechanical changes (in the case of chalking, the loss of coherence of the paint film by oil degradation).

The methods currently used and widely available in the field of conservation science, such as FTIR, are challenging to use as early detection methods due to the unknown 'initial state'. The term 'initial state' in this paper refers to the non-degraded state of the painting, as if it were analyzed immediately after production. When monitoring changes using the current methods, these can be detected but only in relation to a previous state that was analyzed. Furthermore, in the case of FTIR, unambiguous proof of degradation is detectable only when this is also visible by eye[2].

Until today, there is no straightforward analytical method to determine any early warning signs for photocatalytic degradation of unvarnished oil paints containing titanium white, and the methods currently used in the field of conservation are not sufficient to detect this specific process. Therefore, for this paper, new analytical approaches have been explored. In the 20th century, paintings were often unvarnished and unframed [39]. This leads to a lack of protection from the environment as well as a lack of reference material ('initial state'), such as the area protected by the frame. An unknown initial state of the material makes determination of degradation challenging. Once it is clear that photocatalytic degradation is taking place, the object can be completely removed from UV light to stop the degradation. However, it is not feasible, with the exception of some museum collections, to preventively remove UV light everywhere, such as in company art collections that contain large numbers of 20th century works of art [40, 41]. It is therefore important to know which works of art should be protected. For curators and conservators, assessment of paintings is based on visual inspection [42]. A connection between analytical results and a parameter that is related to a common visual observation, is therefore required for good communication with the field of conservation.

In the current paper, we follow the aging of unvarnished titanium white oil paints on the nano-scale with AFM and XPS and we relate this to the macro-scale phenomena of gloss change and chalking. Even though SEM can provide sharper images, AFM offers, as advantage, information about the height profile of the paint sample. On the other hand, XPS is a surface sensitive technique, therefore small changes in elemental composition at the surface of the paint film can be determined. In practice, an oil paint film has a so-called medium skin (see Figure S1[3]), which is a thin layer of unpigmented oil at the surface of the paint film formed during the drying process. The thickness of this layer (t_{ms}) depends on,

[2] Personal experience of the authors during preliminary studies.

[3] Figures labelled 'S' can be found in the supplementary information.

among others, pigment volume concentration (PVC) and manner of application [39]. If this organic layer, composed mainly of carbon, hydrogen and oxygen, is thicker than the penetration depth (d_{xps}) of XPS analysis ($t_{ms} > d_{xps}$), an unaged paint film should show only carbon and oxygen signals in XPS analysis. In this case, the initial situation ($x_{Ti}=0$) is known and fixed which offers a benefit over methods described previously. During aging, the binder is broken down and a titanium signal should appear in the XP Spectra ($x_{Ti}>0$). If this process can be verified for several types of paint, XPS could serve as an early warning detection method for degradation. In this study, the focus is on linseed oil-based paint that serves as a model binder for all types of drying oils.

Combining morphological and elemental information of the paint surface and at the same time connecting this to the macro phenomena of gloss change and chalking will offer insight into the degradation process of oil paints containing photocatalytic titanium dioxide. The insight gained is used to propose a four-step degradation model. Even though XPS and AFM are not common and accessible methods in the field of conservation yet, these techniques may prove their value in the coming years and are therefore put in perspective using a step-by-step method to determine early warning signs for photocatalytic degradation. In the field of conservation, a micro-destructive technique will only be performed if the presence of titanium dioxide in the paint film is confirmed. This can be determined by a non-invasive method such as portable X-ray fluorescence spectroscopy or Raman spectroscopy [2, 43]. Furthermore, the crystal structure of the titanium white could be characterized prior to XPS/AFM investigation. This can be done non- or micro-invasively, depending on the available equipment with X-ray diffraction or Raman spectroscopy [2].

2. Materials & Methods

2.1. Sample preparation

Paint films were prepared by mixing titanium dioxide with linseed oil. Two types of titanium dioxide were used: Hombitan LW, an uncoated anatase (UA) from Sachtleben Chemie, and CR-826, a coated rutile (CR) pigment of the highest durability grade from Tronox. The powders were used as received. The used oil is commercial hot-pressed linseed oil of the brand van Beek. In view of the long drying time of oil paint, a drying agent was used to speed up oil polymerization. The drying agent, a mixture of cobalt and zirconium carboxylates, was obtained from Pieter Keune and used as received[4]. 0.1% v/v was added to 1 L of oil, and the resulting oil was sealed and kept in the dark to prevent polymerization [44]. Paints with a PVC of 15% were prepared by mixing pigment with oil. The mixture was mixed three times for 25 rotations on a glass plated paint mill, an automatic Muller, with a weight of 5 kg. In between mixing, the mixture was scraped together with a palette knife. The paints were spread out on Melinex supports with a draw down bar, applying a fixed layer thickness of 100 µm, and left to dry for 14 days in the lab environment (*T=20°C*, cyclic lighting). The paint with photocatalytic pigment was prepared in duplo (UA-1 and UA-2), since it was expected to show severe degradation. As comparison to the degrading paints, the paint with photostable pigment (CR) was exposed to the same conditions and analyzed using the same techniques.

After drying, the paints were cut into seven fragments of 1 by 2 cm and one larger fragment of 7.5 by 2.5 cm, Figure S2. The larger fragment was used to monitor gloss during the aging process. After the gloss measurement, the large sample was returned to the aging chamber. The small fragments were taken out of the UV chamber at different irradiation

[4] The product is similar to Natural Pigments 500-CZCD02 Cobalt system dryer.

dose and were analyzed using XPS and AFM on multiple spots. Previous experience with aging experiments indicated this would be necessary, because aging is an inhomogeneous process. The samples were aged in an Opsytec Dr. Gröbel BS-02 UV chamber with UV-MAT dose control. The chamber was equipped with UVA lamps. The UV distribution of the UV chamber, provided by the company, is taken into account to calculate the amount of UV received by each sample, as summarized in Table 1.

Table 1: Irradiation dose received by each sample. Maximum irradiation [13387 J/cm^2] is equivalent to 7 years of outdoor exposure. Calculation based on 1.35 W/m^2 UV content on earth [45] and an average of 12 hours of light a day [46].

AFM&XPS samples	***I_0 [J/ cm^2]***	***I_1 [J/ cm^2]***	***I_2 [J/ cm^2]***	***I_3 [J/ cm^2]***	***I_4 [J/ cm^2]***	***I_5 [J/ cm^2]***	***I_6 [J/ cm^2]***	***I_7 [J/ cm^2]***	***LAB, t [h]***
UA-1	0	2115	4231	5261	6346	7267	10883	12704	-
UA-2	0	1662	3324	4134	4845	5548	8309	9698	970
CR	0	1899	3799	4724	6278	7189	10766	12567	970
Gloss samples	***I_0 [J/ cm^2]***	***I_1 [J/ cm^2]***	***I_2 [J/ cm^2]***	***I_3 [J/ cm^2]***	***I_4 [J/ cm^2]***	***I_5 [J/ cm^2]***	***I_6 [J/ cm^2]***	***I_7 [J/ cm^2]***	**LAB, t [h]**
UA-1	0	1705	3411	4241	5391	6173	9245	10791	-
UA-2	0	2115	4231	5261	6687	7658	11468	13387	0-970
CR	0	1985	3972	4939	6278	7189	10766	12567	0-970

After removal from the UV-chamber, samples were kept in the dark until analysis. Dark storage causes yellowing of the oil, which is a property of linseed oil unrelated to the presence of TiO_2 and will therefore not be discussed in this paper [47].

To confirm that the analyzed change is related to UV exposure, paint samples of UA-2 and CR have been kept in the lab environment, parallel to the aging in the UV chamber, for 970 hours (*T=20°C*, cyclic lighting).

2.2. Analysis

Gloss was measured using a Sheen Instruments Ltd Tri-GLOSSmaster. The gloss number is measured at three different angles: 20°, 60° and 85°. Low angles of measurement are commonly used for high gloss, while high angles are more suitable for low gloss measurements. High angle gloss will therefore be discussed in this paper, but all angles have been monitored. The gloss was measured three times per measuring point, with the equipment being repositioned in between the analyses.

AFM analysis was performed using an NT-MDT Ntegra instrument equipped with a silicon Etalon tip. Samples were analyzed at three to five different locations of either 10*10 μm or 20*20 μm. In case of visible sample heterogeneity (Figure S3 and S4), clearly distinct areas (white and yellow) were both analyzed in three to five locations. All samples of UA-1 were imaged, while only the beginning and end stages as well as the sample kept in the lab were selected for imaging for UA-2 and CR. Imaging parameters (force and scan speed) were optimized per image. From the AFM images, the Nova software provides the minimum and maximum recorded height value which was used to calculate the largest height difference in the image, Δz_{max}. For each sample these values were averaged over the three to five recorded images.

XP Spectra were recorded on a K-alpha Thermo Fisher Scientific spectrometer using monochromated Al *Kα* X-ray source. The UA-1 measurements were carried out by using a line scan of four points to account for possible sample heterogeneity, with each point having a spot size of 300 μm at ambient temperature. The chamber pressure was about 10^{-7} mbar.

UA-2 and CR measurements were performed with a line scan of three points. UA-1 line scan locations were oriented on white or yellow areas by using the built-in sample microscope, whereas for the UA-2 and CR samples random locations on the overall yellow paint film were studied (Figure S3). A flood gun was used during data acquisition for charge compensation. All spectra were corrected by setting the reference binding energy of carbon (1**s**) to 284.8 ± 0.1 eV. The electron energy analyzer was operated with a pass energy of 50 eV, and every location was scanned ten times. The spectra were analyzed and processed using Thermo Avantage v5.913 software (Thermo Fisher Scientific). The peaks were fitted using Lorentzian–Gaussian product functions. Smart background subtraction (derived from the Shirley background) was used over the peak width. Relative atomic compositions were calculated using atomic sensitivity factors of 1.000, 2.881 and 6.471 for C1*s* (element), O1s (element) and Ti2*p* (titania), respectively. Atomic composition values reported are averages over at least 2 line scans for titanium and at least 3 line scans for carbon and oxygen.

XPS is a highly surface sensitive technique. The penetration depth is approximated by the inelastic mean free path of crystalline graphite which has a lattice spacing of 3.4 Angstrom and therefore a penetration depth that ranges between 3 to 6 monolayers of graphite or 1-2 nm [48]. Since dried linseed oil is not a well-defined crystal lattice but an amorphous matrix, the penetration depth cannot be determined accurately and is estimated to be between 1 and 5 nm which is the range and slightly larger than the penetration depth for crystalline graphite.

3. Results

3.1. General observations during aging

As expected, inhomogeneity of aging was observed. Intermediate samples of UA-1 (I_4-I_6) had clearly visible yellow and white areas, (Figure S3a and Figure S4). In this case, the white and yellow areas were analyzed separately labeled ‘via yellow’ and ‘via white’ respectively. In gloss measurements, the inhomogeneity is averaged out due to the large measuring area. The difference in color is a result of the various stages in the degradation process. In white areas, the oil binder had decomposed, and consequently it did not produce a yellow color. In the white areas, degradation is visible by eye. Yellow areas were still visibly in an earlier degradation stage and had not started chalking [43]. In yellow areas, degradation is not visible by eye yet. Therefore ‘via yellow’ is of more interest for the determination of early warning signs.

The inhomogeneity of the UA-2 samples was far less pronounced (Figure S3c). The paint film seemed to degrade more gradually and remained yellow until it had reached the point of severe chalking. Therefore, results of UA-2 are not differentiated in yellow and white. As anticipated, the CR samples showed no signs of degradation (Figure S3b), and are treated similarly to UA-2.

3.2. Gloss

Figure 1 shows the gloss results of uncoated anatase and coated rutile aged under UV. A large gloss drop of roughly 50% for the uncoated anatase samples can be observed upon initial exposure to 3000 J/cm^2 UV light. The gloss number quickly stabilizes to a value of around 40 gloss units, showing very slight decrease in gloss for the following 8000 J/cm^2. Partial paint chalking is confirmed after 8000 J/cm^2, however complete chalking of the paint film occurs after 10.000 J/cm^2, indicating that the stabilization stage gradually turns into a

degraded stage. Both stages have similar gloss. Both UA paints follow the same trend confirming inter-sample reproducibility. The low standard deviation of 0.1 to 1.1 gloss units confirms reproducibility of the analysis. The paint containing the photostable pigment (CR) does not show any change in gloss during UV exposure (Figure 1). The same holds for the paints exposed to the lab environment.

Figure 1: 85 degree gloss during UV exposure. Error bars are included in the plot, however the error is small and therefore not visible.

3.3. AFM

Figure 2 shows a selection of the AFM images of sample UA-1. A z-scale development from 100 to 2000 nm can be seen upon UV exposure in the uncoated anatase samples. In the initial stage, the z-scale varies between 25 and 250 nm in relatively continuous patterns. Upon UV light irradiation, the paint films quickly become rougher and the patterns become increasingly discontinuous. After 2000 J/cm^2 of UV light, the z-scale has risen 5-fold, and after 5000 J/cm^2 the z-scale reads 1600 nm, nearly reaching the maximum obtained value of 2000 nm at 12.000 J/cm^2. The same trend is demonstrated in Figure 3, where the maximum height difference is plotted (Δz_{max}). Again, the largest change is detected at the beginning of the aging process until roughly 6500 J/cm^2. The stabilized stage merges into the chalking stage beyond values of 10.000 J/cm^2. The *via white* curve stabilized earlier, confirming the general observation that white areas have reached the chalking stage at the end of the degradation process. The photostable reference (CR), illustrated in Figure S5 and Figure 3, shows high stability in the height difference during irradiation. The same holds for the sample kept in the lab environment as illustrated in Figure S6.

Figure 2: 2D AFM images of UA-1

Figure 3: Δz_{max} averaged over 3 to 5 AFM scanning areas.

3.4. XPS

XPS survey spectra of UA-1 are shown in Figure 4a; the total survey spectrum is shown in Figure S7a. The observed signals in the survey spectra are identified as C1*s* (284.8 eV), Ti2*p* (485.8 eV) and O1*s* (532.4 eV). In the initial I_0 sample, only carbon and oxygen signals are present. This remains the case in samples I_2 and I_3: after more than 5200 J/cm^2 of irradiation, there is no clear signal for titanium. The spectra for I_4 differ from the previous ones: a clear Ti contribution can be distinguished around 458.8 eV. The specific binding energies of the Ti2$p_{3/2}$ (458.8 eV) and Ti2$p_{1/2}$ (464.5 eV) signals confirm the oxidized nature of the titanium species. The Ti peak intensity is further enhanced for samples I_5 to I_7, indicating that increasing amounts of TiO_2 are located on the surface of the paint. The Ti3*s* (59 eV) and Ti3*p* (33 eV) peaks now become visible as well. The relative atomic concentration of Ti on the surface was quantitatively assessed and plotted together with the relative atomic concentrations of C and O in Figure 4b. The error bars (similar to Figure 6b) are due to the sample heterogeneity and the averaging of multiple analysis spots. Two lines are plotted for the Ti content, differentiating between yellow and white areas. These differences for the oxygen and carbon signals are incorporated in the error of the measurements of the intermediate samples. The results show that Ti is not detected on the

surface unless the paint is exposed to over 6000 J/cm^2 of UV irradiation (I_4). A steep rise in the Ti signal is observed, reaching a value of around 10 at% for the white area. The value for the yellow areas remains lower for the entire range until the sample has chalked completely.

The relative atomic content of carbon decreases (figure 4b), while the relative amount of titanium is increasing as more binder decomposes to reveal the white pigment. Core-level spectra of titanium (Figure 5a) show the evolution of the Ti signal with irradiation in more detail. Where the survey spectra could not reveal the minor amount of Ti on the surface, the core-level spectra display the onset of Ti surfacing in samples I_2 and I_3. These subtle, but significant changes may prove valuable as early warning signs. From sample I_4 onwards, the full Ti signal is well defined and it confirms a huge increase in Ti surface concentration. As a consequence, the oxygen content increases as well, since for every atom of titanium, two atoms of oxygen will reach the surface. This increase is clearly displayed in Figure 5b, allowing differentiation between the oxygen originating from the organic matrix and the oxygen from the metal oxide source. The binding energy for the metal oxide is shifted roughly 3 eV to lower binding energy, confirming unambiguously the presence of titanium white on the paint surface. Core-level spectra of carbon are displayed in Figure S7b.

To investigate the degradation of the paint in more detail, UA-2 paint films were analyzed with XPS, since the overall yellow paint film seemed to degrade more gradually and homogenously. Survey spectra of UA-2 samples are displayed in Figure 6a (total survey in Figure S8) with the relative atomic composition in Figure 6b. Certainly, from both the spectra and atomic content it can be seen that the onset period is far better defined. The results suggest that only after more than 5500 J/cm^2 (I_5) Ti is starting to surface on the entire paint film. The value of the Ti atomic content then quickly rises to above 9 at%.

XPS analysis of CR shows high stability of the survey spectrum during irradiation (Figure S9). The characteristic Ti contribution is not detected in any of the spectra. The same is true for samples aged under lab conditions.

Figure 4: a) Survey spectra of UA-1 paint film samples in various stages of degradation. b) Atomic composition of UA-1 paint film during aging, differentiating between white and yellow areas.

Figure 5: Core-level XPS spectra of titanium a) and oxygen b) in UA-1 paint film in various stages of degradation.

Figure 6: a) Survey spectra of UA-2 paint film samples in various stages of degradation. b) Atomic composition of UA-2 paint film during aging.

4. Discussion

4.1. Gloss, AFM and XPS

Both gloss and AFM analysis show a steep change in the initial stages of degradation for paints containing uncoated anatase. The gloss results stabilize around 3000 J/cm^2, the AFM stabilization occurs somewhat later around 6000 J/cm^2 due to the higher level of detail that can be measured by this technique. The similar trend observed in both techniques can be explained by the changes taking place at the surface of the paint film: they are of

morphological nature. The close relation between gloss and AFM results is confirmed by correlating gloss versus Δz_{max}, obtaining a linear fit with an R^2 of 0.84 (Figure 7).

Figure 7: Correlation plot 85 degree gloss and Δz_{max} (AFM). Values of degradation 'via-yellow' of sample UA-1 are used.

In the XPS results of uncoated anatase, Ti only significantly surfaces after 6000 J/cm^2 for both UA-1 and UA-2 samples. Below 6000 J/cm^2, there is hardly any change in the XPS spectra (<0.5 At% Ti), in contrast to AFM and gloss results. The shift in analysis difference is closely related to the elemental nature of the XPS technique and its penetration depth. To demonstrate that the elemental changes are not random, but related to absolute differences in the paint films, the fully-averaged Ti content for UA-1 and UA-2 samples are compared in Figure 8. The large errors indicated by the error bars are the result of averaging the heterogeneity of paint samples. Nevertheless, the two very similar samples show a near-equal behavior for the entire range of irradiation. These results confirm that XPS is capable of determining the onset in elemental change when paint degradation is imminent. Core-level spectra of high resolution more clearly show the signals of these early warning signs. The Ti2*p* spectra provide valuable information regarding the onset of Ti surfacing, and O1*s* spectra allow for unambiguous identification of TiO_2 species due to the rising shoulder around 529 eV [44].

Figure 8: Ti content on paint film as determined by XPS for UA-1 and UA-2 samples. Large error is due to heterogeneity of paint films.

The results indicate that the various stages of degradation possess certain resemblances and contrasts. The first stages of degradation cause a large morphological change (surface roughness), which is followed by a large change in elemental composition (Ti surfacing), finally resulting in a dramatic mechanical change (chalking). Both the morphological change and the elemental stage follow a rather steep trend. The different changes require analysis by different surface analysis techniques.

In general, AFM is less sensitive to disturbances such as dust/paint strokes than gloss measurement. Furthermore, on a real object it is hard to find a large enough area to measure gloss. Finally, the gloss measurement is mostly valuable as comparative data over time, therefore knowing the initial situation is necessary. For this reason, we propose to use AFM imaging as confirmation of the situation as assessed by XPS and as an indication of the stage before TiO_2 surfacing. Nevertheless, the relation to real gloss change will be an important factor in the communication with conservators.

Paints containing the photostable pigment show high stability in all analytical techniques. This is an indication that no other effects apart from photocatalytic degradation cause the change observed in the paints containing photocatalytic pigments. It confirms that an inorganic coating is a very effective way to reduce the photocatalytic activity of titanium white pigments [2, 11-13].

Paints that were not exposed to such high doses of UV light (being kept in the lab environment) also showed high stability during the employed timeframe (970 h of cyclic low intensity light) in all analytical techniques. The results of these lab references confirm the process of UV-initiated photocatalysis, which is caused by the size of the bandgap of titanium dioxide [2]. It has been shown that the photocatalytic degradation rate scales with the square root of the intensity [49]. This suggests that degradation will inevitably take

place but that the monitored 970 h with very low exposure compared to high-powered UV light of the lamps correspond to only a very small irradiation dose in the UV chamber.

Other (white) pigments may show degradation processes based on soap formation and pigment migration [50-51], but it is unlikely that this is the case here for several reasons. Boundary conditions for pigment migration include the reaction of the pigment with the binding medium or free fatty acids, the dissolution of the pigment in the binding medium or in free fatty acids, and a driving force causing the movement (such as a concentration gradient). There is no reason to assume UV light could be a driving force for migration. If migration would play a role, both lab-aged and UV-aged samples should show similar effects and this is not the case. Furthermore, it is well known no solvents for titanium dioxide are available [52]. If dissolution would occur, both anatase and rutile samples would be expected to show changes and this is not the case.

4.2. Proposed model for photocatalytic degradation of titanium dioxide oil paints

Based on the different results and previous knowledge of photocatalytic degradation, we propose the model illustrated in Figure 9 for photocatalytic degradation of oil paint. It is known that photocatalytic degradation proceeds via the absorption of UV light by the titanium white pigments. This leads to the production of highly reactive radicals that can break down the oil binding medium into small volatile components such as CO_2 and H_2O [53,54]. This type of severe binder degradation leads to an effect called chalking, when the pigment is no longer bound by the binding medium [18]. We propose that this process happens in four stages: the intact paint film (stage 1), the initial oil breakdown (stage 2), the TiO_2 surfacing (stage 3) and the chalked paint film (stage 4). Between stage 1 and 2 the largest morphological change occurs at the surface, causing optical changes such as a strong decrease of gloss. This decrease in gloss, even though it is strong, can sometimes be difficult to assess because the initial gloss is not known. After the morphological change stabilizes, between stage 2 and 3, and the medium skin is thinner than the XPS penetration depth, titanium dioxide starts to be detected by XPS. This is the early warning sign that degradation is taking place. Depending on the location of the measurement this sign can be detected in stage 2 or it can be determined unambiguously in stage 3. Finally, between stage 3 and 4 the real damage occurs: dramatic mechanical change leading to a completely chalked paint film.

Figure 9: Proposed model of linseed oil degradation mechanism in relation to gloss, AFM and XPS analysis.

4.3. Method for detection of early degradation signs for photocatalytic degradation

A first step in the investigation of possible photocatalytic degradation of unvarnished oil paint is confirming the presence of titanium dioxide. Without this knowledge, no micro-destructive method would be considered. There are several ways to confirm the presence of titanium dioxide by none-invasive techniques, the most straightforward being to use a portable XRF instrument (e.g. Bruker Tracer) [55]. In the field of conservation, this technique is often used as a 'point and shoot' method [56]. The presence of the element titanium is mostly related to titanium dioxide. However, care should be taken for instance with respect to the overlap of Ti *K* lines with Ba *L* lines in XRF analysis. Also the use of filters, adjusting the X-ray source for background reduction and speciation to a specific element need to be taken into account when performing XRF analysis. Furthermore, interpretation of the results is

always complex due to the unknown layer structure of a painting, especially because grounds also often consist of white pigments [43].

When the presence of titanium dioxide is confirmed, the crystal structure should be determined either non-invasively by portable Raman spectroscopy or micro-invasively by XRD of a micro sample. If the high risk anatase crystal structure is found, a sample for XPS and AFM analysis should be taken. The presence of the rutile crystal structure indicates a lower risk of degradation. However this risk is not zero: it has been shown that several rutile pigments have lower but not negligible photocatalytic activity [14]. A sample for XPS and AFM preferably has the largest possible size acceptable to conservators with a minimum XPS spot size of 50 μm. With a larger spot size XPS resolution is increased. Taking a surface sample and transporting it without damaging the surface is a practical challenge that still needs to be faced. Since AFM may disturb the sample surface, XPS analysis should be performed first. It is important to use both AFM and XPS since AFM may detect roughening before XPS detects titanium dioxide. AFM has a less clear initial state than XPS analysis (x_{Ti} = 0), nevertheless, a height difference of more than 250 nm (Δz_{max} > 250 nm) is a clear indication of initial degradation. All paints containing coated rutile or paints aged in the lab environment had Δz_{max} distances varying between 20 and 250 nm depending on variations during paint application and drying. This is considered to be the unaged reference and therefore an indication of the range of the initial state for AFM. If it is found that photocatalytic degradation is occurring, the object should be removed from UV light to stop the degradation process and prevent severe mechanical damage.

5. Conclusions

A combined study of loss of gloss, AFM and XPS analysis was performed on the surface of model paints containing titanium white. The photocatalytic degradation of the oil paint was successfully mapped using these techniques, and reference material confirmed that photocatalysis initiated by titanium white is responsible for paint degradation. It was found that AFM and XPS are suitable techniques to monitor paint aging at the surface and that new and valuable information can be gained about changes occurring during the aging process. Combined XPS and AFM analysis is a strong method to detect early degradation in these types of paint. Both techniques offer a fixed initial state (x_{Ti} = 0, Δz_{max} < 250 nm, respectively) making them particularly useful for the field of conservation science. For investigation of real works of art and the application of the proposed step-by-step method of determining early warning signs of degradation, the sampling technique needs to be optimized. Surface samples of a minimum spot size of 50 μm and preferably a larger spot size, for enhanced resolutions, are required.

Based on the analysis, a four-stage model of the degradation process was proposed. Initial degradation (stage 2) of the intact paint film (stage 1) causes the biggest morphological change. This can be monitored by AFM analysis. After the initial breakdown, extensive titanium white surfacing occurs as a result of bulk oil binder degradation (stage 3). At this point, the dramatic mechanical changes leading to chalking (stage 4) have not yet taken place, and the method can therefore be used as an early warning sign for degradation.

The work presented here shows that, provided proper micro sampling can be performed, combined application of AFM and XPS analysis is a promising approach to detect early photocatalytic degradation in titanium white containing oil paints. Furthermore, the combination of methods offers valuable insight and a better understanding of the steps in the degradation process.

Acknowledgements
This work is supported by AkzoNobel and accommodated by the Rijksmuseum. The authors would like to thank Ing. Marcel Bus, ChemE, Delft University of Technology, for his assistance with the AFM analysis. The Automatic Muller is on permanent loan from Old Holland to the Cultural Heritage Institute of the Netherlands.

Symbols

t_{ms} = thickness medium skin
d_{xps} = penetration depth of XPS analysis
x_{Ti} = atomic composition Titanium
PVC = Pigment volume concentration = ($V_{pigment}/V_{total}$)*100)
Δz_{max} = maximum height difference per AFM image
d_{min} = minimal diameter of a paint sample usable for AFM and XPS investigation
d_{pref} = preferred diameter of a paint sample usable for AFM and XPS investigation
T = lab temperature

References

1. Michalski, S. (1997). *The lighting decision*.
2. M. Laver (1997). Chapter 10: Titanium white. In E.W. Fitzhugh (Ed.), *Artists' Pigments: Volume 3: A Handbook of their History and Characteristics* (pp. 295-355). National Gallery of Art. DOI: 10.2307/1506685
3. van den Berg, K.J., Miliani, C., Aldrovandi, A., Brunetti, B. G., de Groot, S. , Kahrim, K., . . . van Bommel, M. R. (2012). Chapter 7: The Chemistry of Mondrian's paints in Victory Boogie Woogie. In M. R. van Bommel, H. Janssen, R. Spronk & Het Gemeentemuseum (Eds.), *Inside Out Victory Boogie Woogie*. Amsterdam: Amsterdam University Press. ISBN: 9789089643735
4. Cooper, H., Spronk, R., Museums, Harvard University Art Museums and Dalles Museum of Art. (2001). *Mondrian: the Transatlantic Paintings*: Yale University Press. ISBN: 9780300089288
5. Thorn, A. (2000). Titanium dioxide: a catalyst for deterioration mechanisms in the third millennium. *Stud Conserv,* 45(Supplement-1), 195-199. doi: doi:10.1179/sic.2000.45
6. Lauridsen, C. B., Sanyova, J., & Simonsen, K. P. (2014). Analytical study of modern paint layers on metal knight shields: The use and effect of Titanium white. *Spectrochim Acta A,* 124, 638-645. doi: http://dx.doi.org/10.1016/j.saa.2014.01.077
7. de Keijzer, M., de Groot, S., Megens, L., & Van Keulen, H. (2008). *Schildertechnisch onderzoek aan Mondriaans Compositie met rood, zwart, geel en grijs uit 1920*. Instituut collectie Nederland.
8. Sclafani, A., & Herrmann, J. M. (1996). Comparison of the Photoelectronic and Photocatalytic Activities of Various Anatase and Rutile Forms of Titania in Pure Liquid Organic Phases and in Aqueous Solutions. *J. Phys. Chem.,* 100(32), 13655-13661. doi: 10.1021/jp9533584
9. Zhang, J., Zhou, P., Liu, J., & Yu, J. (2014). New understanding of the difference of photocatalytic activity among anatase, rutile and brookite TiO2. *Phys. Chem. Chem Phys.,,* 16(38), 20382-20386. doi: 10.1039/C4CP02201G
10. Kim, W., Tachikawa, T., Moon, G.-h., Majima, T., & Choi, W. (2014). Molecular-Level Understanding of the Photocatalytic Activity Difference between Anatase and Rutile Nanoparticles. *Angew. Chem. Int. Ed.,* 53(51), 14036-14041. doi: 10.1002/anie.201406625
11. Day, R. E., & Egerton, T. A. (1987). Surface studies of TiO2 pigment with especial reference to the role of coatings. *Colloids Surf.,* 23(1–2), 137-155. doi: http://dx.doi.org/10.1016/0166-6622(87)80255-X

12. de Keijzer, M. (2002). *The history of modern synthetic inorganic and organic artists' pigments*: James & James (Science Publishers) Ltd.
13. Allen, A. (1979). TiO2 pigment coated with dense silica and porous alumina/silica. Patent US4075031 A.
14. van Driel, B.A., et al. (2016), *A quick assessment of the photocatalytic activity of TiO2 pigments — From lab to conservation studio!* Microchem J, 126**,** 162-171.
15. Blakey, R.R. (1980), *The role of Titanium dioxide in the protection of Paint Media*. Technical Service Report Tioxide
16. Spathis, P., Karagiannidou, E., & Magoula, A.-E. (2003). Influence of Titanium Dioxide Pigments on the Photodegradation of Paraloid Acrylic Resin. *Stud Conserv,* 48(1), 57-64. doi: 10.2307/1506823
17. [Personal communication Bert Klein-Ovink from Royal Talens.] (2014).
18. Völz Hans, G., Kaempf, G., Fitzky Hans, G., & Klaeren, A. (1981). The Chemical Nature of Chalking in the Presence of Titanium Dioxide Pigments. In F.H. Winslow (Ed.) *Photodegradation and Photostabilization of Coatings, Acs symposium series* (Vol. 151, pp. 163-182). American Chemical Society.
19. Linsebigler, A. L., Lu, G., & Yates, J. T. (1995). Photocatalysis on TiO2 Surfaces: Principles, Mechanisms, and Selected Results. *Chem. Rev., 95*(3), 735-758. doi: 10.1021/cr00035a013
20. Fujishima, A., Rao, T. N., & Tryk, D. A. (2000). Titanium dioxide photocatalysis. *J. Photochem. Photobiol. C,* 1(1), 1-21. doi: 10.1016/S1389-5567(00)00002-2
21. Johnston-Feller, R., Feller, R. L., Bailie, C. W., & Curran, M. (1984). The Kinetics of Fading: Opaque Paint Films Pigmented with Alizarin Lake and Titanium Dioxide. *JAIC,* 23(2), 114-129. doi: doi:10.1179/019713684806028269
22. Samain, L., Silversmit, G., Sanyova, J., Vekemans, B., Salomon, H., Gilbert, B., . . . Strivay, D. (2011). Fading of modern Prussian blue pigments in linseed oil medium. *J. Anal. At. Spectrom.,* 26(5), 930-941. doi: 10.1039/C0JA00234H
23. Zhang, A. (2013). *Photocatalytical Effect of TiO2 pigments on the surface of Paint films*. Master thesis Materials Science and Engineering, Delft university of Technology. Retrieved from http://repository.tudelft.nl/view/ir/uuid%3A940a74cf-2f11-45af-a4d5-d66218632535/
24. Yousif, E., & Haddad, R. (2013). Photodegradation and photostabilization of polymers, especially polystyrene: review. *SpringerPlus,* 2(1), 398.
25. Kampf, G., Papenroth, W., Voltz, G., & Weber (1982), G. Time-lapse observation of Chalking under the electron microscope. 16th FATIPEC Congress Proceedings, 3, 167-174
26. Pappas, S. P., & Fischer, R. M. (1975). Photo-chemistry of pigments. Studies on the mechanism of chalking. *Pigm. Resin Technol.,,* 4(1), 3-10. doi: 10.1108/eb041057
27. Colling, J. H., & Dunderdale, J. (1981). The durability of paint films containing titanium dioxide — Contraction, erosion and clear layer theories. *Prog. Org. Coat.,* 9(1), 47-84. doi: http://dx.doi.org/10.1016/0033-0655(81)80015-5
28. Shang, J., Chai, M., & Zhu, Y. (2003). Solid-phase photocatalytic degradation of polystyrene plastic with TiO2 as photocatalyst. *J. Solid State Chem.,* 174(1), 104-110. doi: http://dx.doi.org/10.1016/S0022-4596(03)00183-X
29. Zhao, X. u., Li, Z., Chen, Y., Shi, L., & Zhu, Y. (2007). Solid-phase photocatalytic degradation of polyethylene plastic under UV and solar light irradiation. *J. Catal. A.,* 268(1–2), 101-106. doi: http://dx.doi.org/10.1016/j.molcata.2006.12.012
30. Allen, N. S., Edge, M., Ortega, A., Sandoval, G., Liauw, C. M., Verran, J., . . . McIntyre, R. B. (2004). Degradation and stabilisation of polymers and coatings: nano versus pigmentary titania particles. *Polym. Degrad. and Stabil.*, 85(3), 927-946.
31. Gaumet, S., Siampiringue, N., Lemaire, J., & Pacaud, B. (1997). Influence of titanium dioxide pigment characteristics on durability of four paints (acrylic isocyanate, polyester melamine, polyester isocyanate, alkyd). *Surf. Coat. Int.,* 80(8), 367-372. doi: 10.1007/BF02692692
32. de Sá, M. H., Eaton, P., Ferreira, J. L., Melo, M. J., & Ramos, A. M. (2011). Ageing of vinyl emulsion paints—an atomic force microscopy study. *Surf. Interface Anal.,* 43(8), 1160-1164. doi: 10.1002/sia.3664

33. Gesenhues, U. (2000). Influence of titanium dioxide pigments on the photodegradation of poly(vinyl chloride). *Polym. Degrad. Stab.*, 68(2), 185-196. doi: http://dx.doi.org/10.1016/S0141-3910(99)00184-6
34. Izzo, F. C., Zendri, E., Biscontin, G., & Balliana, E. (2011). TG–DSC analysis applied to contemporary oil paints. *J. Therm. Anal. Calorim.,* 104(2), 541-546. doi: 10.1007/s10973-011-1468-y
35. Lazzari, M., & Chiantore, O. (1999). Drying and oxidative degradation of linseed oil. *Polym. Degrad. Stab.,* 65(2), 303-313. doi: http://dx.doi.org/10.1016/S0141-3910(99)00020-8
36. Spyros, A., & Anglos, D. (2004). Study of Aging in Oil Paintings by 1D and 2D NMR Spectroscopy. *Anal. Chem,* 76(17), 4929-4936. doi: 10.1021/ac049350k
37. van den Berg, J. D. J. , van den Berg, K.J., & Boon, J. J. (1999). Chemical changes in curing and ageing oil paints. *Paper presented at the ICOM Committee for Conservation.*
38. Bonaduce, I., Carlyle, L., Colombini, M. P., Duce, C., Ferrari, C., Ribechini, E., . . . Tine, M. R. (2012). New Insight into the ageing of linseed oil paint binder: A Qualitative and Quantitative analytical study. *Plos ONE, 7*(11). doi: 10.1371/journal.pone.0049333
39. Burnstock, A., de Keijzer, M., Krueger, J., Learner, T., de Tagle, A., Heydenreich, G., & van den Berg, K. J. (2014). *Issues in Contemporary Oil Paint* (pp. 11). Springer International Publishing.
40. Vereniging Bedrijfscollecties Nederland. Retrieved 25-09-2015, 2015, from http://www.vbcn.nl/
41. [Personal communications with representatives of several Dutch company art collections] (2015).
42. [Personal experience during contact with conservators] (2014-2015).
43. Namowicz, C., Trentelman, K., & McGlinchey, C. (2009). Erratum: XRF of cultural heritage materials: Round- Robin IV --- Paint on Canvas. *Powder diffr.,* 24, 124-129. doi: DOI: 10.1154/1.3132591
44. Boyatzis, S., Ioakimoglou, E., & Argitis, P. (2002). UV exposure and temperature effects on curing mechanisms in thin linseed oil films: Spectroscopic and chromatographic studies. *JAPS,* 84(5), 936-949. doi: 10.1002/app.10117
45. Wikipedia, Sunlight Retrieved 28-08-2015, from https://en.wikipedia.org/wiki/Sunlight
46. Amsterdam climate. Retrieved 28-8-2015, from http://www.amsterdam.climatemps.com/sunlight.php
47. Mallégol, J., Lemaire, J., & Gardette, J.-L. (2001). Yellowing of Oil-Based Paints. *Stud. Conserv.,* 46(2), 121-131. doi: 10.2307/1506842
48. Lüth, H. (1993), *Surfaces and interfaces of solids*. Springer-Verlag.
49. Egerton, T. A., & King, C. J. (1979). The influence of light intensity on photoactivity in TiO2 pigmented systems. *J. Oil Col. Chem. Assoc, 62*, 386-391.
50. Osmond, G. (2012), *Zinc white: a review of zinc oxide pigment properties and implications for stability in oil-based paintings.* AICCM Bulletin, 33(1), 20-29.
51 Higgitt, C., M. Spring, and D. Saunders (2003), *Pigment-medium Interactions in Oil Paint Films containing Red Lead or Lead-tin Yellow.* National Gallery Technical Bulletin, 24, 75-95
52 Diebold, M.P., et al. (2004), *Rapid assessment of TiO2 pigment durability via the acid solubility test.* JCT Research, 1(3), 239-241.
53 Jin, C., et al. (2006). *Rapid measurement of polymer photo-degradation by FTIR spectrometry of evolved carbon dioxide.* Polym. Degrad. Stab. 91(5): 1086-1096. DOI: http://dx.doi.org/10.1016/j.polymdegradstab.2005.07.011
54 Christensen, P. A., et al. (1999). *Infrared spectroscopic evaluation of the photodegradation of paint Part I The UV degradation of acrylic films pigmented with titanium dioxide.* J. Mater. Sci. 34(23): 5689-5700. DOI: 10.1023/A:1004737630399
55 Palmer, D. P. *Introduction to energy-dispersive x-ray fluorescence (XRF) - an analytical chemistry perspective* Presentation. Department of chemistry & biochemistry San Francisco state university Retrieved from http://www.google.nl/url?sa=t&rct=j&q=&esrc=s&source=web&cd=1&ved=0CDIQFjAA&url=http%3A%2F%2Fwww.asdlib.org%2FonlineArticles%2Fecourseware%2FPalmer%2FASDL%2520Intro%2520to%2520XRF.pdf&ei=5XHsU5fSMsTZPI72gMAO&usg=AFQjCNGOh7qSMPZIWk7GbulddRg620KOQ
56 SRAL. (2015). Portable X-Ray Fluorescence Spectroscopy Conference and Workshop. Retrieved 24-09-2015, 2015, from http://www.sral.nl/nl/nieuws/portable-x-ray-fluorescence-spectroscopy-conference-and-workshop/

FIG1_1Column_PPTX

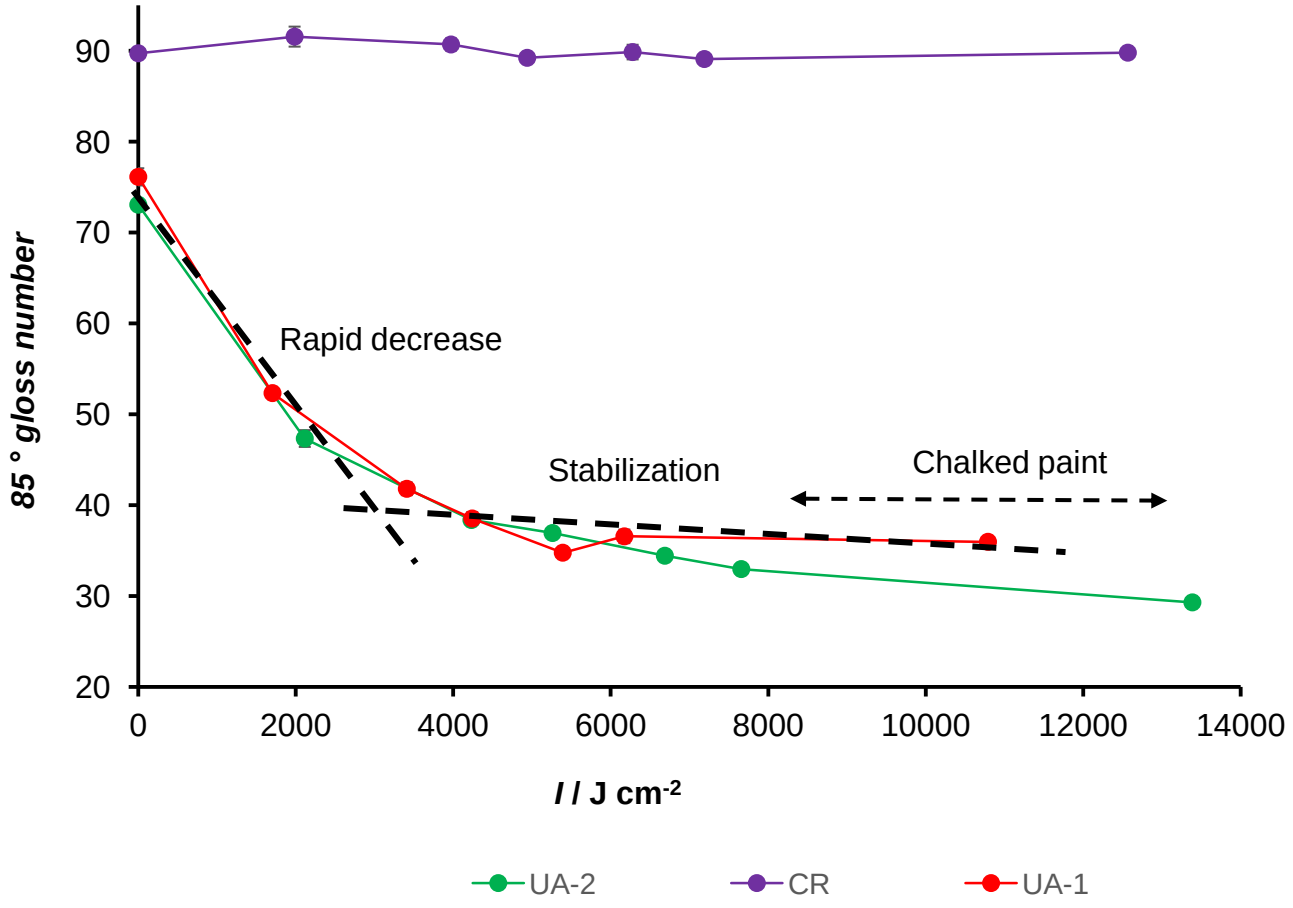

FIG2_2Column_revised.JPEG

Click here to download high resolution image

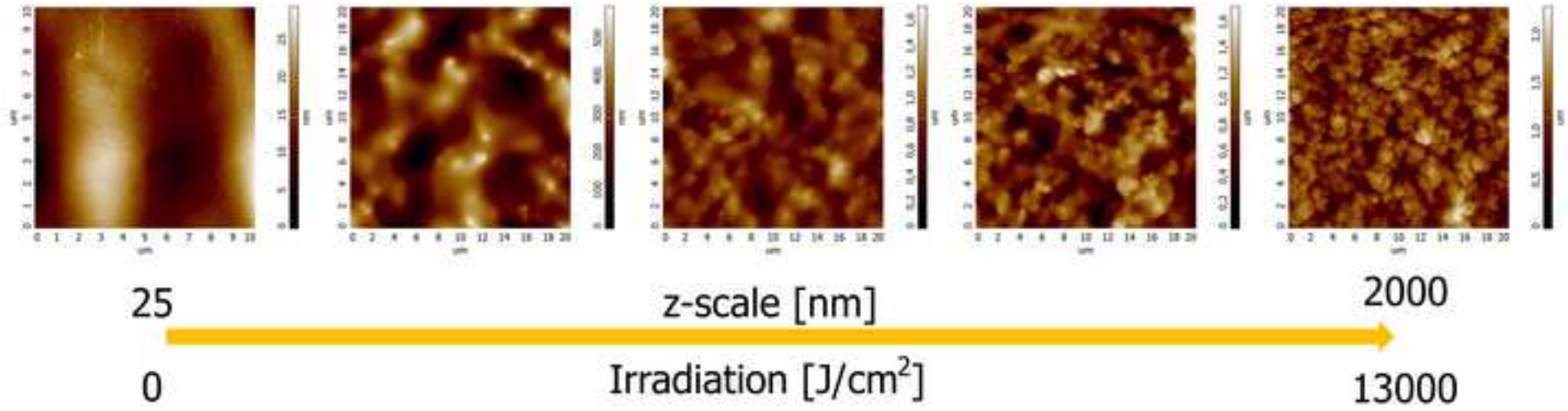

FIG3_1Column_revised.PPTX

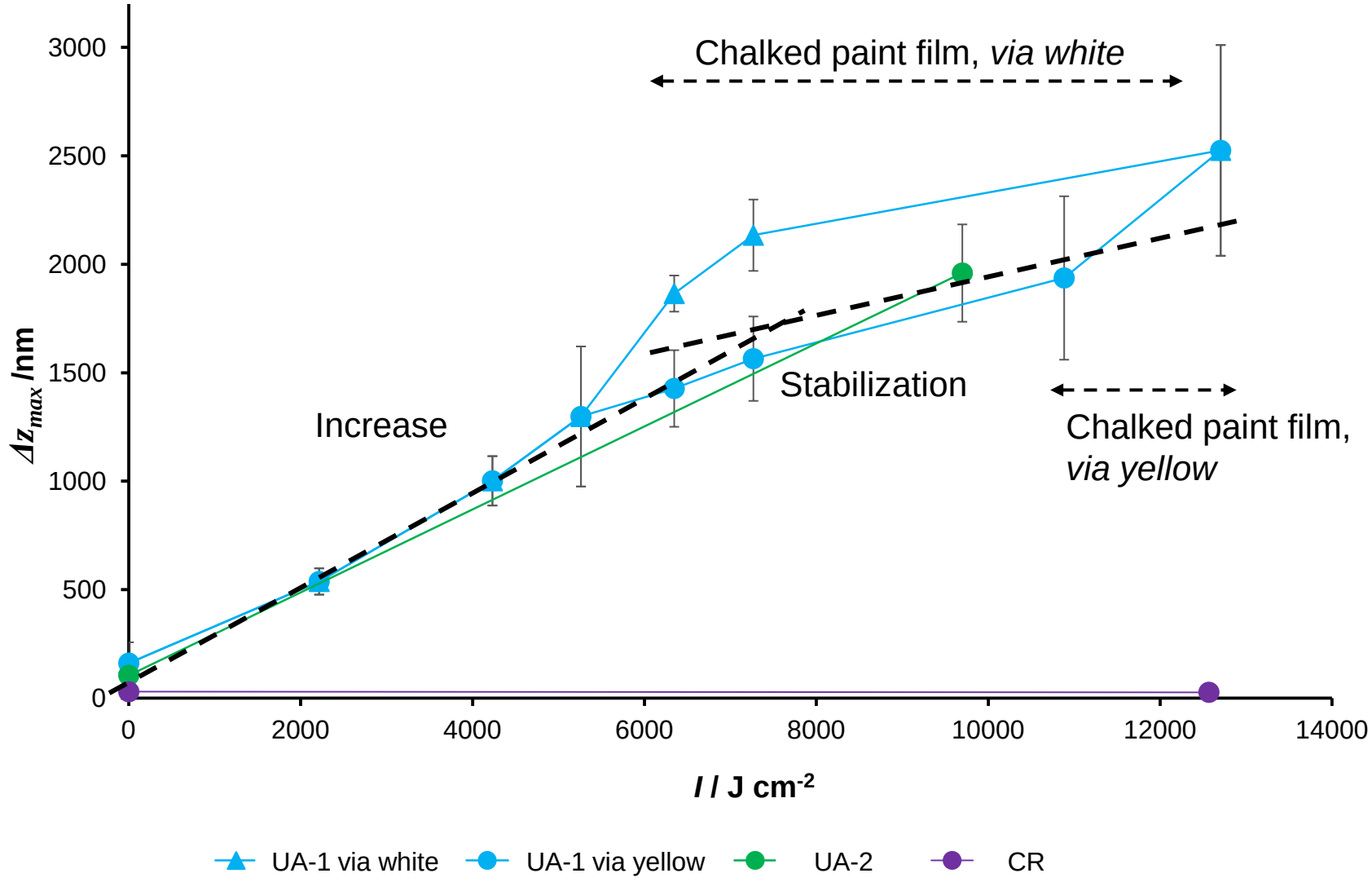

FIG4_2Column.JPEG

Click here to download high resolution image

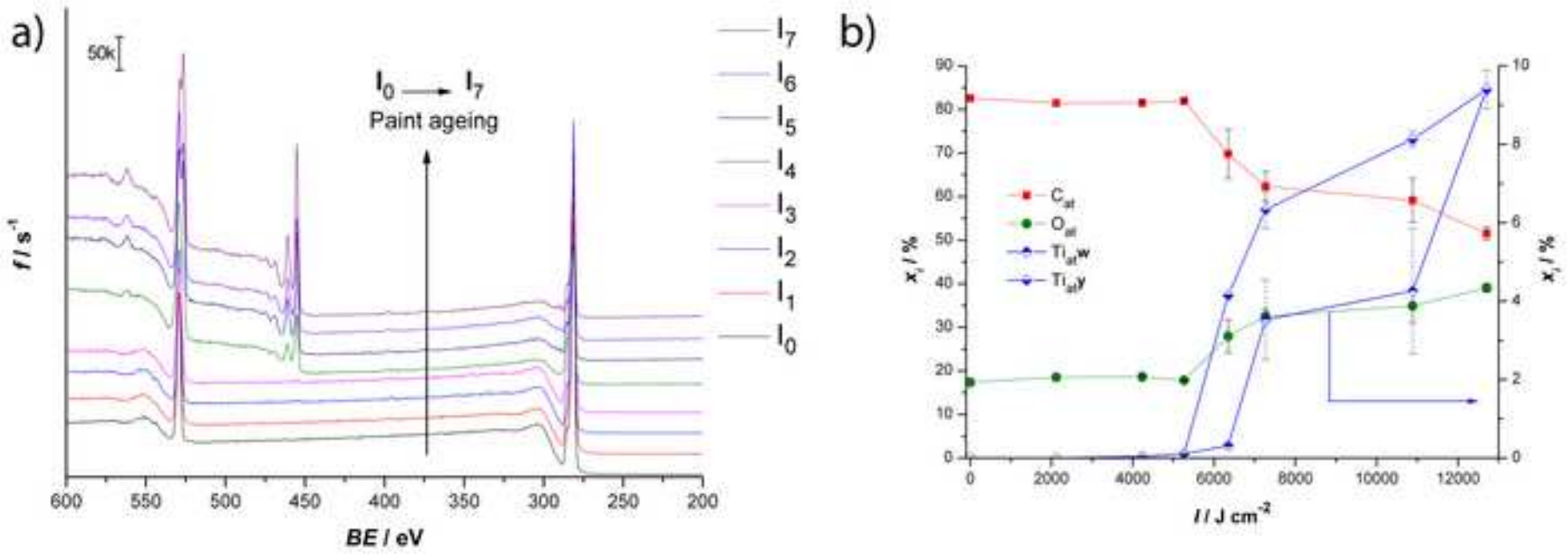

FIG5_2Column.JPEG

Click here to download high resolution image

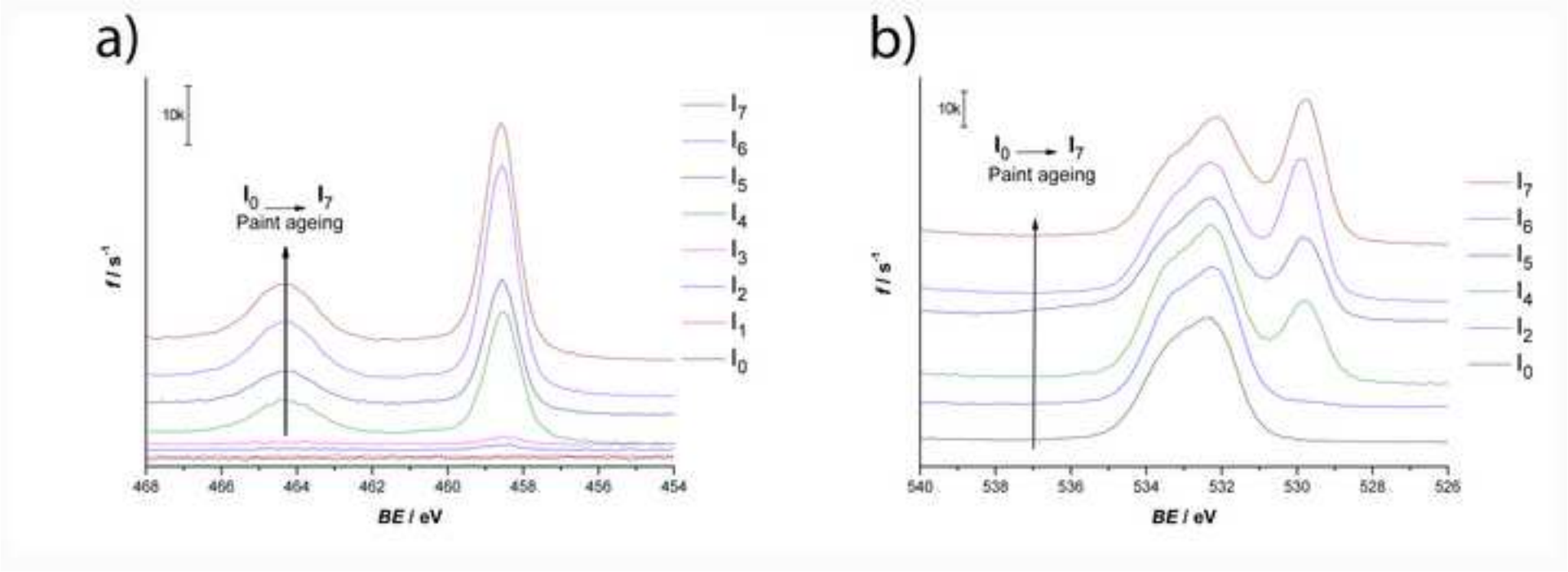

FIG6_2Column.JPEG

Click here to download high resolution image

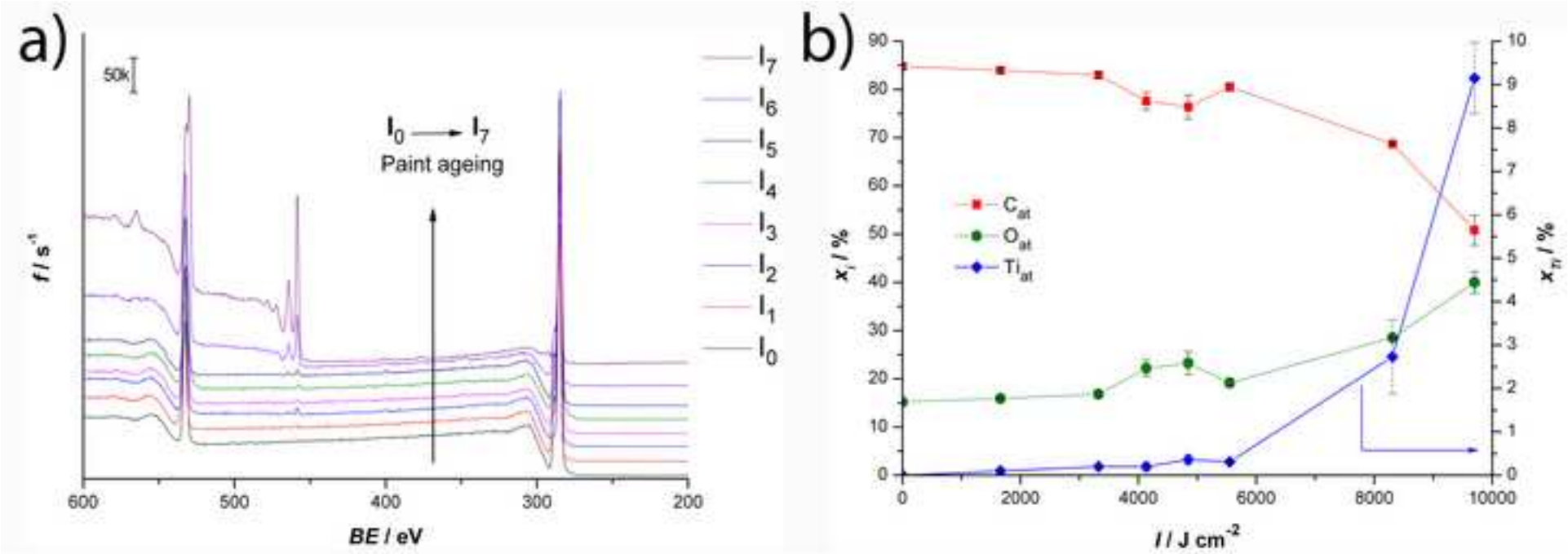

FIG7_1Column_revised,PPTX

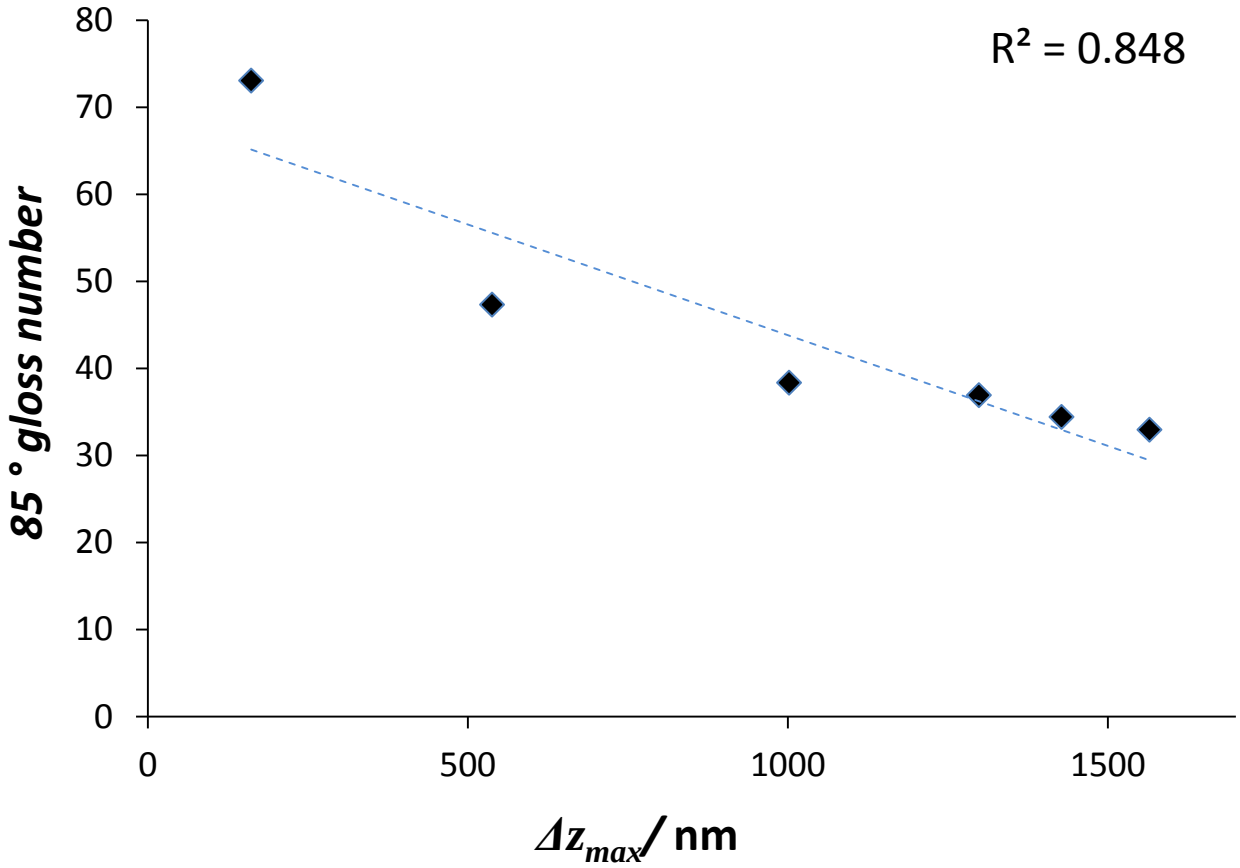

FIG8_1Column.JPEG

Click here to download high resolution image

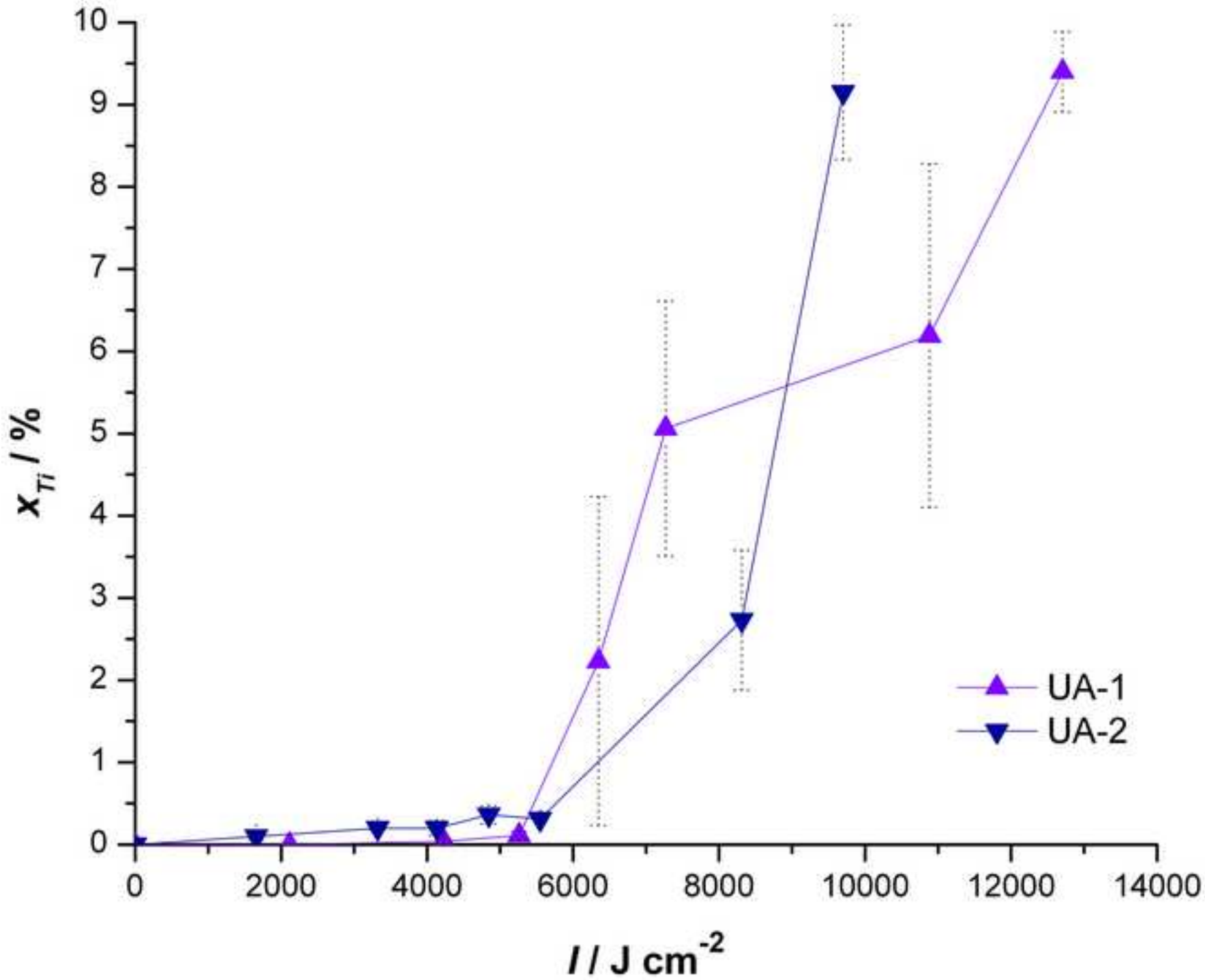

FIG9_2Column.PPTX